Direct in vivo V_H to J_H rearrangement violating the 12/23 rule

Sergei B. Koralov,[1] Tatiana I. Novobrantseva,[1] Konrad Hochedlinger,[2] Rudolf Jaenisch,[2] and Klaus Rajewsky[1]

[1]The CBR Institute for Biomedical Research, Harvard Medical School, Boston, MA 02115
[2]Whitehead Institute for Biomedical Research, Cambridge, MA 02142

V(D)J recombination at the immunoglobulin heavy chain (IgH) locus follows the 12/23 rule to ensure the correct assembly of the variable region gene segments. Here, we report characterization of an in vivo model that allowed us to study recombination violating the 12/23 rule, namely a mouse strain lacking canonical D elements in its IgH locus. We demonstrate that V_H to J_H joining can support the generation of all B cell subsets. However, the process is inefficient in that B cells and antibodies derived from the D_H-less allele are not detectable if the latter is combined with a wild-type IgH allele. There is no preferential usage of any particular V_H gene family or J_H element in V_HJ_H junctions, indicating that 23/23-guided recombination is possible, but is a low frequency event at the IgH locus in vivo.

CORRESPONDENCE
Klaus Rajewsky:
rajewsky@cbr.med.harvard.edu

B and T cell antigen receptor genes are assembled from variable (V), diversity (D), and joining (J) segments in a process termed V(D)J recombination. V(D)J recombination requires the lymphoid-specific proteins RAG1 and RAG2 as well as ubiquitous DNA repair factors. The coding sequences of V, D, and J gene segments are flanked by recombination signal sequences (RSSs). Each RSSs consists of a highly conserved heptamer and a nanomer separated by a spacer of either 12 or 23 base pairs (1).

V(D)J recombination is initiated by the introduction of DNA double-strand breaks at one 12 RSS and one 23 RSS by RAG1/2. The coding segments are fused to produce a coding joint and the RSS are assembled to create a signal joint. In the murine IgH locus, the V and J elements are flanked by RSSs with a 23-bp spacer and the D elements are flanked on both sides by RSSs with a 12-bp spacer, thus insuring that direct V_H to J_H joining does not occur. As a rule, the segments to be recombined are flanked by RSSs of dissimilar length. This phenomenon, referred to as the 12/23 rule, ensures correct assembly of VDJ joints (2).

In vitro assays by Gellert et al. (3) as well as other groups (4, 5) have demonstrated a strong preference for dissimilar partners regardless of whether the RAG/DNA synapse formation begins at a 12 or at 23 RSS. However, although incorporation of a similar RSS partner was undetectable when RAG1/2 was assembled on the 12 RSS, incorporation of a 23-RSS compared with a 12-RSS partner was only sixfold reduced when synapse formation was initiated on the 23 RSS (3).

We turned our attention to a mouse cloned from the nucleus of a lymph node B cell (6) in search of an in vivo model for V_H replacement, a process in which a new V_H element "invades" and replaces the V_H element used in a rearranged V(D)J joint. The B cell nucleus that gave rise to this mouse contained two rearranged IgH alleles, one of which was in-frame. The other IgH locus was nonproductively rearranged, carrying an elusive rearrangement that could not be characterized using standard PCR for VDJ/DJ joint amplification. In the course of identifying the nature of this rearrangement, we were surprised to find an IgH locus lacking canonical D_H elements. Although this allele is not suited to analyze V_H replacement, it provides a unique opportunity to study possible exceptions to the 12/23 rule of VDJ recombination at the IgH locus in vivo. Indeed, D_H-less mice generate small numbers of B cells whose IgH chains likely result from direct V_H to J_H joining.

S.B. Koralov and T.I. Novobrantseva contributed equally to this work.

T.I. Novobrantseva's present address is Biogen Idec, Inc., Cambridge, MA 02142.

The Journal of Experimental Medicine

RESULTS AND DISCUSSION

Characterization of the nonproductive IgH gene rearrangement in the LN1 mouse

We set out to identify the nature of the nonproductive rearrangement in the mouse generated from a LN B cell (LN1) by means of a genomic PCR walk (see Materials and Methods) because standard PCR approaches using cocktails of V_H and D_H gene-specific primers and primers 3′ of the J_H elements did not allow us to amplify this rearrangement (6). We identified a rearrangement that used the J_H1 element and a sequence immediately upstream of DFL16.1 (Fig. 1). Because DFL16.1 is the most 5′ canonical D_H element in the mouse, this rearrangement deletes all the D_H elements on the corresponding IgH allele. In addition, the J_H1 element is no longer available for further rearrangements because its RSS is deleted. However, the other three J_H elements are retained, roughly 98 kb downstream of the most 3′ V_H segment. The newly identified allele structure predicts the pattern seen in the Southern analyses describing the LN1 mouse in the original publication (6). We termed this IgH allele ΔD and mice homozygous for ΔD D_H-less.

The nucleus of the B lymphocyte from which Hochedlinger and colleagues (6) succeeded to clone a mouse had acquired an irregular D_H to J_H joining event on one of its IgH alleles, leading to the inappropriate joining of a sequence upstream of DFL16.1 to J_H1, rather than joining that D_H element to J_H1 in inverted orientation. Although such an event is probably rare in B cell development, we see no reason why it should have conferred a selective advantage to the nucleus carrying this rearrangement with respect to its ability to allow nuclear cloning. Therefore, we consider the fact that this particular joining event was present in the B cell nucleus from which the mouse was cloned to be a fortunate coincidence, allowing us to study B cell development in mice lacking canonical D_H elements in their IgH locus.

D_H-less mice are capable of generating B cells

In 5-wk-old D_H-less mice, B cells are readily detectable and represent ∼5% compared with ∼55% of splenocytes in WT animals. Absolute splenic B cell numbers are ∼34-fold reduced at this age (Fig. 2 A). In 6-mo-old animals, we saw a significant accumulation of B cells to ∼22% of total splenocytes in mutants versus 56% in WT, with absolute numbers of B cells only approximately sevenfold reduced compared with WT (Fig. 2 A). These data are consistent with a low rate of B cell production and mature B cell accumulation with age, and correspond to what is observed in other mouse mutants with impaired B cell production (7). Analyzing mice at the age of 2–3 wk, we observed a ∼40-fold reduction in B cell numbers (unpublished data).

Marginal zone (MZ) B cells and B1 cell fractions are enlarged in D_H-less mice

Based on the CD23/CD21 staining pattern, $CD19^+CD21^{int}$ $CD23^{hi}$ follicular (B2) cells were more strongly reduced in the spleens of the mutant animals than MZ B cells (Fig. 2 A). The number of $CD19^+CD21^{hi}CD23^{lo}$ MZ B cells increased more than sevenfold from weeks 5 to 25, whereas the increase was less than threefold in control mice. A similar accumulation of MZ B cells has been observed earlier in mice with low rates of B cell generation such as mice lacking the λ5 gene product or both λ5 and κ light chains (unpublished data) and other mouse mutants (8, 9). The B1a ($CD5^+CD19^{hi}$) and B1b ($CD5^-CD19^{hi}$) cell populations were not reduced as dramatically as B2 cells in D_H-less compared with WT mice, with virtually no reduction in the peritoneal cavity (Fig. 2 C) and an approximately fivefold reduction in the spleen of 5-wk-old mice. B1 cells have been ascribed a self-renewing capacity (10) and this may also pertain to the MZ subset (8).

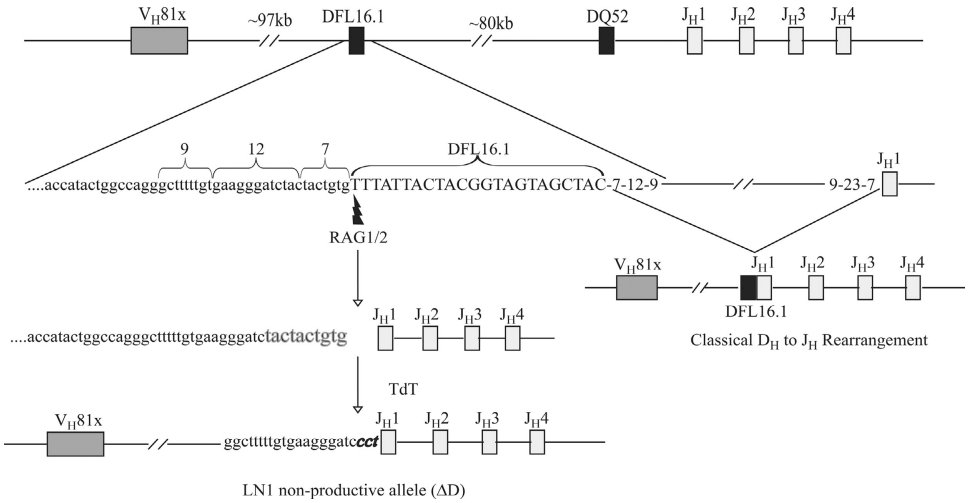

Figure 1. LN1 nonproductive allele structure. Configurations of wild type and LN1 nonproductive (ΔD) IgH loci are depicted together with proposed intermediates. Nucleotides inserted during the ΔD rearrangement are highlighted in italics and nucleotides that are lost in the process of rearrangement are shaded. The ΔD rearrangement may be the result of incorrect resolution of the RAG–DNA complex that results in J_H1 joining the sequence upstream of the DFL16.1 instead of the DFL16.1 in an inverted orientation.

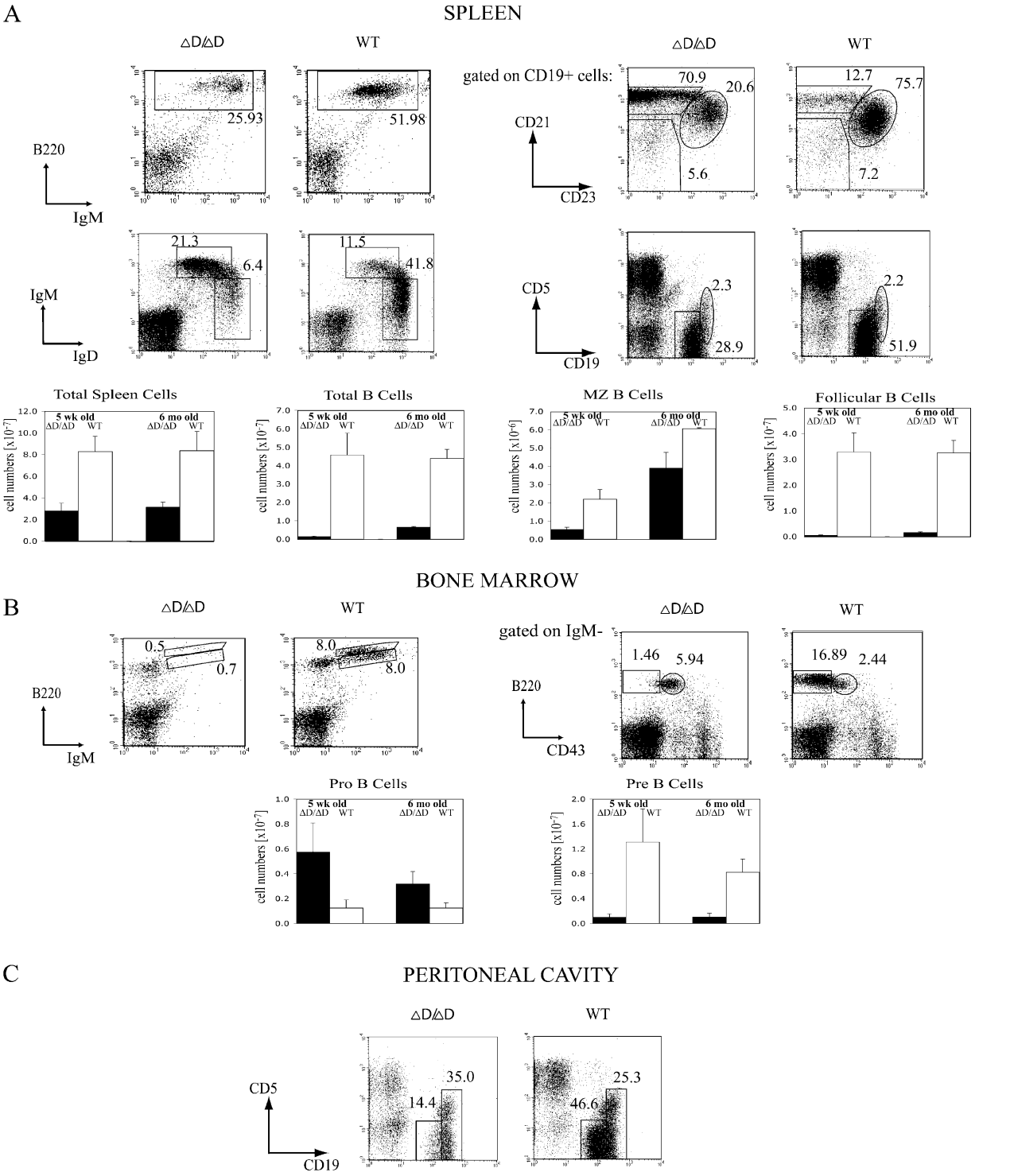

Figure 2. ΔD/ΔD mice generate all peripheral B cell subsets with a low rate of B cell production. Representative flow cytometric analyses of lymphocytes in spleen (A), bone marrow (B), and peritoneal cavity (C) of ΔD/ΔD and WT mice. Shown are cells in the "lymphocyte gate" unless additional gates are specified. Numbers within the FACS plots indicate the percent of cells that fall into a given gate. For spleen (A) and bone marrow (B), average values and standard deviations are shown for different B cell subsets. ΔD/ΔD mice are represented by closed bars, and WT mice by open bars. $n = 6$ for 5-wk-old ΔD/ΔD mice, $n = 4$ for 5-wk-old WT mice, $n = 3$ for 6-mo-old ΔD/ΔD mice, and $n = 2$ for 6-mo-old controls. Representative FACS plots shown in the figure are for 6-mo-old mice.

Most B cell progenitors are blocked at the pro– to pre–B cell transition in D_H-less mice

Consistent with the low rate of B cell generation, we detected a block at the pro– to pre–B cell transition with accumulation of $IgM^-B220^+CD43^+$ pro–B cells (Fig. 2 B) in the bone marrow. Only those developing B lymphocytes that receive a signal from a pre–B cell receptor are selected into the pre–B cell compartment (for review see reference 9). Thus, the observed blockade at this developmental stage likely reflects the low probability of generating a gene encoding a functional heavy chain by direct V_H to J_H joining. There is an approximately eightfold decrease of $IgM^-B220^+CD43^-$ pre–B cells compared with controls, and IgM^+B220^{hi} mature recirculating B cells are hardly detectable in the BM of mice homozygous for the ΔD allele (Fig. 2 B).

Homozygous but not heterozygous mutant mice produce cells and antibodies derived from the ΔD allele

In an attempt to compare the efficiencies of classical VDJ recombination and the aberrant joining that occurs at the ΔD allele in a competitive situation, we generated heterozygous mutant mice, with the WT IgH allele of the *a* allotype from the BALB/c strain. The D_H-less allele is derived from the C57BL/6 mice and, thus, is of the *b* allotype (6). B cells of the IgM^b allotype were virtually undetectable in these animals and, in the serum, IgM antibodies of the *b* allotype were also essentially absent (Fig. 3). In mice homozygous for the ΔD allele, the levels of IgM were similar to those of controls (Fig. 3), whereas the levels of IgG1 were fivefold lower and those of IgA two times higher than in ΔD/+ mice (not depicted).

Joints formed at the IgH allele in the D_H-less mouse show direct V to J joining

To analyze the gene rearrangements in the IgH locus that allowed for the production of B cells in D_H-less mice, we examined the sequences of V_H to J_H joints in homozygous D_H-less mice or $\Delta D/J_HT$ mice. The J_HT allele is not able to encode IgH chains because it lacks J_H elements (11). We amplified IgH rearrangements from the B cells of these mice using three different approaches: PCR with single cell DNA as a template, followed by direct sequencing (12) as well as RT-PCR using RNA from FACS-purified B cells and PCR using DNA from magnetic-activated cell sorting (MACS)-purified B cells followed by cloning and sequencing (see Materials and Methods). Fig. 4 depicts sequences obtained by these three approaches, with joints amplified by RT-PCR shown in detail (Fig. 4 A) and the fractions of productive and nonproductive rearrangements for the two DNA-based methods (Fig. 4 B). 66 out of 71 recombination products in the D_H-less mice were likely resulting from direct V_H to J_H joining. However, five joints used a single, previously identified putative D_H element, DST4.2 (13), which is still present in the ΔD allele. In the sequence between VH81X and DFL16.1 (as currently available from Ensembl), we found only two pairs of inverted heptamers that are separated by <150 bp: DST4.2, which is flanked by poorly conserved RSSs, and another 10-bp-long sequence flanked by canonical heptamers but lacking recognizable nanomers (GenBank/EMBL/DDBJ accession no. AY841982). We did not detect any remnants of this 10-bp sequence in any of the 71 sequences. We screened all stretches of N/P nucleotides of six bases or more in our sequences against the 97-kb germline sequence between VH81X and DFL16.1 to make sure that they did not reappear in the sequence flanked by sequences resembling heptamers and found no such case. All three J_H elements remaining in the ΔD allele and a spectrum of V_H gene families were used in our sequence collection (Fig. 4 A). We analyzed the RSSs of the V_H genes used in the 66 sequences likely reflecting direct V_H to J_H joining and found that the distance between canonical heptamers and nanomers of these V_H genes was 22–23 nucleotides with no sequence resembling a nanomer in the spacer (unpublished data). We conclude that the process allowing the formation of a productive joint on the ΔD allele in 66 out of the 71 sequences is likely direct recombination between V_H and J_H elements, both flanked by 23 RSSs.

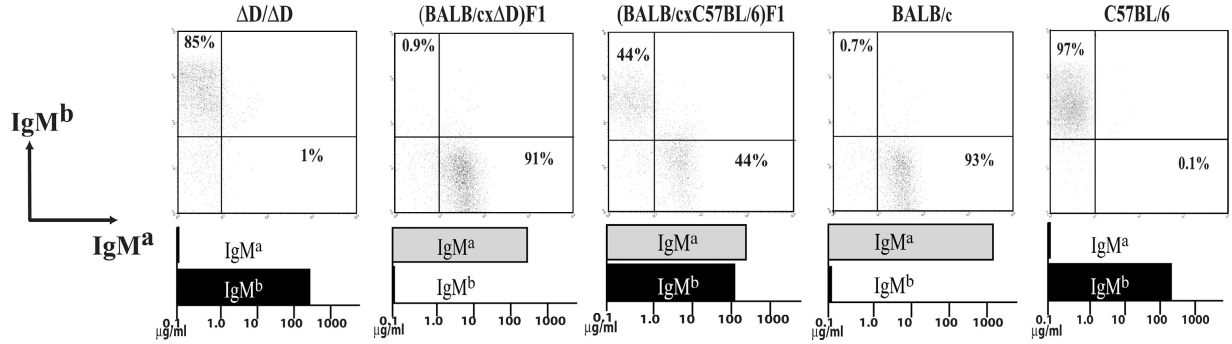

Figure 3. The ΔD allele cannot compete with the WT allele in either B cell generation or antibody production. FACS analysis of CD19-gated splenocytes from 5-mo-old ΔD/ΔD, (BALB/c × ΔD)F1, (BALB/c × C57BL/6)F1, C57BL/6, and BALB/c mice for the expression of IgM of *a* and *b* allotypes. The ΔD allele is of the *b* allotype, the IgH loci of BALB/c and C57BL/6 mice are of the *a* and *b* allotype, respectively. Bar graphs below the FACS plots summarize the ELISA data with serum IgM levels plotted in μg/ml for 10-wk-old mice ($n = 2$ for each group). Gray bars represent IgM of the *a* allotype and black bars IgM of the *b* allotype.

In the 66 V_HJ_H joints, we observed an average of ~3 P and N nucleotide insertions per junction (Fig. 4), compatible with a single recombination event (14, 15). We found that the CDR3 regions amplified from the ΔD/ΔD B cells are shorter than the WT CDR3s, and that this reduction in length corresponds to the average number of nucleotides inserted in one round of N and P nucleotide addition and the average length of a D_H sequence in WT $V_HD_HJ_H$ joints (Fig. 4 C). Looking at V_HJ_H junctions from 2-, 5-, and 10-wk-old mice, no obvious selection over time of cells expressing antibodies with longer CDR3s became apparent. Among the sequences amplified from the DNA of B cells from homozygous mutant mice, we detected only a single, potentially nonproductive joint with a stop codon in the V_H gene segment in 39 analyzed sequences from ΔD/ΔD B cells. All other joints were productive. In contrast, out of 71 joints amplified from WT B cells, we found 24 to be nonproductive, either due to out-of-frame joining or stop codons in the joint (Fig. 4 B). From this, we conclude that direct recombination between V_H and J_H elements is a rare event in vivo, as cells that have acquired a nonproductive $V_HD_HJ_H$ joint on one allele and proceeded to rearrange the second allele are apparently missing or very rare in the ΔD/ΔD mice.

Inefficiency of V_H to J_H joining is likely the main explanation for the ΔD allele deficiency

Mice carrying the ΔD allele at both IgH loci show a severe block of B cell development at the pro–B to pre–B transition, but small numbers of B cells were generated, and these B cells expressed IgH chains that resulted from direct V_H to J_H joining as demonstrated by sequence analysis of the corresponding gene rearrangements. All subsets of mature peripheral B cells were detectable in D_H-less mice. Therefore, D_H elements are not essential for the generation of antibody specificities that drive follicular, MZ, or B1 cell differentiation (16).

However, strikingly, the ΔD allele was unable to successfully compete with a WT IgH locus in heterozygous mutant mice in the generation of the antibody repertoire. In these animals, essentially all B cells expressed IgH chains encoded by the WT IgH locus, and there were almost no antibodies with IgH chains encoded by the ΔD allele present in the blood. One reason for the almost complete absence of cells expressing the ΔD allele is clearly the inefficiency of V_H to J_H joining, as is apparent from the block in B cell development in homozygous mutant mice and the almost exclusive presence of productive V_HJ_H joints in the B cells generated in these animals. The latter finding indicates that the mutant cells do not have sufficient time in development to undergo successive rearrangements at the two homologous IgH loci. Given this situation, it is expected and indeed experimentally found (Fig. 3) that B cells expressing the WT rather than the mutant IgH locus vastly outnumber cells expressing the ΔD allele in heterozygous mutants. B cells expressing the WT allele may have an additional advantage in populating the peripheral immune system in that they express a broader repertoire of antibody specificities. However, even in the bone marrow, immature B cells expressing the ΔD allele are hardly detectable in the heterozygous mutant mice (Fig. 5). Therefore, inefficiency of V_H to J_H joining is apparently the main cause of the inability of the ΔD allele to compete with a WT IgH allele in vivo.

MATERIALS AND METHODS

Cloning of the nonproductive IgH gene rearrangement from the LN1 mouse. Genomic DNA was prepared from LN1 ES cells (6) using the Genomic DNA Kit according to the manufacturer's instructions (QIAGEN). To isolate the unknown sequence fused to the J_H region in the nonproductively rearranged IgH allele of the LN1 mouse, a "pan"-PCR genome walking strategy was performed using adaptor AP1 and adaptor specific primers A1 and A2 (GenomeWalker Kit; CLONTECH Laboratories, Inc.) as described in the original publication by the inventors (17). The gene-specific primers JH4E and JH4A have been described previously (12). The resulting amplification product of 1.7 kb in length was cloned and sequenced to reveal a rearrangement that used the J_H1 element and a sequence immediately upstream of DFL16.1 (Fig. 1).

Preparative and analytical FACS and MACS. Fluorescence staining was performed as described previously (18). Antibodies were conjugated to FITC, PE, APC, PerCP, Cy-Chrome, or biotin. Biotinylated antibodies were developed with streptavidin conjugated to Cy-Chrome or PerCP. Stained cells were analyzed on a FACScalibur (Becton Dickinson). Cell sorting was performed using a triple laser flow cytometer (FACSVantage; Becton Dickinson). Single splenic B and T cells were directly deposited into PCR 96-well plates containing 20 μl 1× PCR buffer (2.5 mM $MgCl_2$; GIBCO BRL), immediately frozen on dry ice, and stored at −80°C. Single cells from the E14 embryonic stem cell line (19) were isolated in a similar way as negative controls for the PCR. Beads were used to confirm that one cell only was deposited in a microtiter plate well; this was further confirmed by the fact that we never saw more than two rearrangements per well in sorted WT B cells.

For bulk analysis, 5×10^4 splenic B cells were sorted into TRIzol (Invitrogen)-containing tubes. T cells from the same cell suspension were sorted in a similar manner as negative controls for the analyses of IgH gene rearrangements.

In a separate experiment, CD19 MACS beads and LS columns (Miltenyi Biotec) were used to separate B cells from whole spleens. The purity of the cells was assessed by B220/CD19 staining. The resulting cell populations contained 90–96% B cells. Mice were kept according to Harvard guidelines.

Single cell PCR. To prepare DNA for amplification, 1 μl of an aqueous solution of proteinase K (10 mg/ml; Boehringer) was added to frozen single cell containing tubes and samples were overlaid with paraffin oil and incubated for 30 min at 55°C. Subsequently, proteinase K was inactivated for 10 min at 95°C. PCR amplification was performed in two rounds: the first reaction contained a mix of all V_H family specific primers and the JH4E primer (12). Amplification was performed over 30 cycles (1 min at 95°C, 1 min at 60°C, and 2.5 min at 72°C). For the second round of amplification, 1.5-μl aliquots of the product of the first round were transferred into separate reactions (set up in 96-well microtiter plates), each containing 7 pmol of a single 5′ primer in combination with 7 pmol of the nested JH4A primer (13). 30 cycles were performed (1 min at 95°C, 1 min at 63°C, and 1.5 min at 72°C). All PCRs contained dATP, dCTP, dGTP, and dTTP (Amersham Biosciences) at 200 μM each, PCR buffer (Eppendorf), 2.5 mM Mg^{2+}, and 5 U Taq DNA polymerase (Eppendorf) in the first round, and 3 U in the second round. The final volume of each reaction was 50 μl. Each PCR was followed by a 5–10-min incubation at 72°C. 10 μl of the second-round PCR product was analyzed on agarose gels. Before sequencing, 1.5 μl of second-round product was reamplified for 20 cycles (30 s at 95°C, 1 min at 63°C, and 2 min at 72°C) using appropriate 5′ primers and nested 3′ primers. Se-

A Joints amplified from bulk RNA

Seq. #	V_H family	V gene segment	N and P nucleotide additions	J_H element	
original LN1 allele		.tggccagggcttttttgtgaagggatc	...cct...	tacttcgatgtctggggc...	Jh1
				AC TAC TTT GAC TAC TGG GGC...	**Jh2**
1	*Vh6*	...TAC TGT GTG AGA	C	AC TAC TTT GAC TAC TGG GGC...	Jh2
2	*Vh6*	...TAC TGT GTG AGA	G	AC TAC TTT GAC TAC TGG GGC...	Jh2
3	*Vh14*	...TAC TGT GCT	GAC	TAC TTT GAC TAC TGG GGC...	Jh2
4*	*Vh7*	...TAC TGT GCA AGA	TGG CAC AGC TCG GG	C TTT GAC TAC TGG GGC...	Jh2
5	*Vh4*	...TAC TGT GTG AGA	CAT G	AC TAC TTT GAC TAC TGG GGC...	Jh2
6[1]	*Vh6*	...TAC TGT GTG AGA	CAT AGG G	AC TTT GAC TAC TGG GGC...	Jh2
7	*Vh2*	...TAC TGT GCC AGA	C	AC TAC TTT GAC TAC TGG GGC...	Jh2
8[2]	*Vh5*	...ACT TGT GCA AGA	CAT G	AC TAC TTT GAC TAC TGG GGC...	Jh2
9[2]	*Vh1*	...TTC TGT	GCA A	AC TAC TTT GAC TAC TGG GGC...	Jh2
10	*Vh1*	...TAC TGT GCA AGA	G	AC TAC TTT GAC TAC TGG GGC...	Jh2
11[2]	*Vh10*	...TAC TGT GTG AGA	C	AC TAC TTT GAC TAC TGG GGC...	Jh2
12	*Vh10*	...TAC TGT GTG AGA	CAT GC	C TAC TTT GAC TAC TGG GGC...	Jh2
13[1]	*Vh1*	...TTC TGT GCA A	AC	TAC TTT GAC TAC TGG GGC...	Jh2
				CC TGG TTT GCT TAC TGG GGC...	**Jh3**
14*	*Vh5*	...TAC TGT GCA AG	G CAC AGC TCG GGC TA	C TGG TTT GCT TAC TGG GGC...	Jh3
15[1]	*Vh1*	...TTC TGT GCA AGA		TTT GCT TAC TGG GGC...	Jh3
16	*Vh10*	...TAC TGT GTG	NAG G	TT GCT TAC TGG GGC...	Jh3
17	*Vh6*	...TAC TGT	CTG AGG	TTT GCT TAC TGG GGC...	Jh3
18	*Vh14*	...TAC TGT ACT	GCC AGG	TTT GCT TAC TGG GGC...	Jh3
19[2]	*Vh1*	...TAC TGT GCA AGA	G	GG TTT GCT TAC TGG GGC...	Jh3
20[2]	*Vh1*	...TTC TGT GCA AGA		TGG TTT GCT TAC TGG GGC...	Jh3
21	*Vh1*	...TTC TGT GCA AGA		TTT GCT TAC TGG GGC...	Jh3
22	*Vh1*	...TTC TGT GCA A	GC C	GG TTT GCT TAC TGG GGC...	Jh3
23	*Vh1*	...TTC TGT GCT ANA		TGG TTT GCT TAC TGG GGC...	Jh3
24	*Vh14*	...TAC TGT GCT AGA	AAC CCT	TTT GCT TAC TGG GGC...	Jh3
25	*Vh1*	...TTC TGT GCA AGA		TTT GCT TAC TGG GGC...	Jh3
26	*Vh1*	...TAC TGT GCA A		GG TTT GCT TAC TGG GGC...	Jh3
27	*Vh1*	...TAC TGT GCA AGA		TGG TTT GCT TAC TGG GGC...	Jh3
28*	*Vh14*	...TAC TGT GCT A	CA GCT CGG GCT A	CC TGG TTT GCT TAC TGG GGC...	Jh3
				AT TAC TAT GCT ATG GAC TAC TGG GGT...	**Jh4**
29	*Vh1*	...TTC TGT GCA		ATG GAC TAC TGG GGT...	Jh4
30[2]	*Vh2*	....TAC TGT GCC AGA	C	AT GCT ATG GAC TAC TGG GGT...	Jh4
31[1]	*Vh10*	....TAC TGT GTG AGA	C	AT GCT ATG GAC TAC TGG GGT...	Jh4
32	*Vh5*	....TAC TGT GCC AGA	C	AT GCT ATG GAC TAC TGG GGT...	Jh4

B Analysis of VH joints amplified from the DNA of single B cells or B cell populations

	total # of joints analyzed	# of non-productive joints
analysis of ΔD/ΔD B cells	39	1
analysis of WT B cells	72	24

C Analysis of CDR3 length

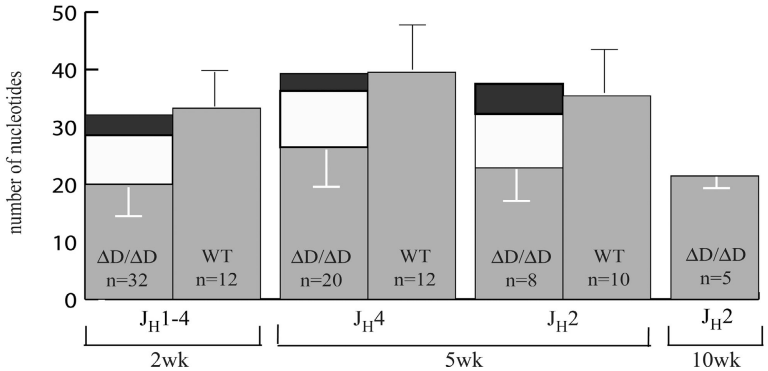

Figure 4. Analysis of IgH V region joints derived from B cells in ΔD mice. (A) Alignment of joints amplified from the RNA of 2-wk-old ΔD/ΔD and ΔD/JHT mice. The joints are shown from the codon immediately 5′ of the second cystein (position 104) of the V_H gene and extending to the conserved glycine of the J_H region. Sequences labeled with an asterisk use the putative D_H element, DST4.2 (underlined). The sequences were analyzed using the http://www.DNAPLOT.de, http://www.imgt.cines.fr, or http://www.ncbi.nlm.nih.gov/igblast websites. In the analysis of bulk-sorted cells, some sequences were found repeatedly, as indicated by the superscripts next to the sequence numbers. As we did not observe repeated

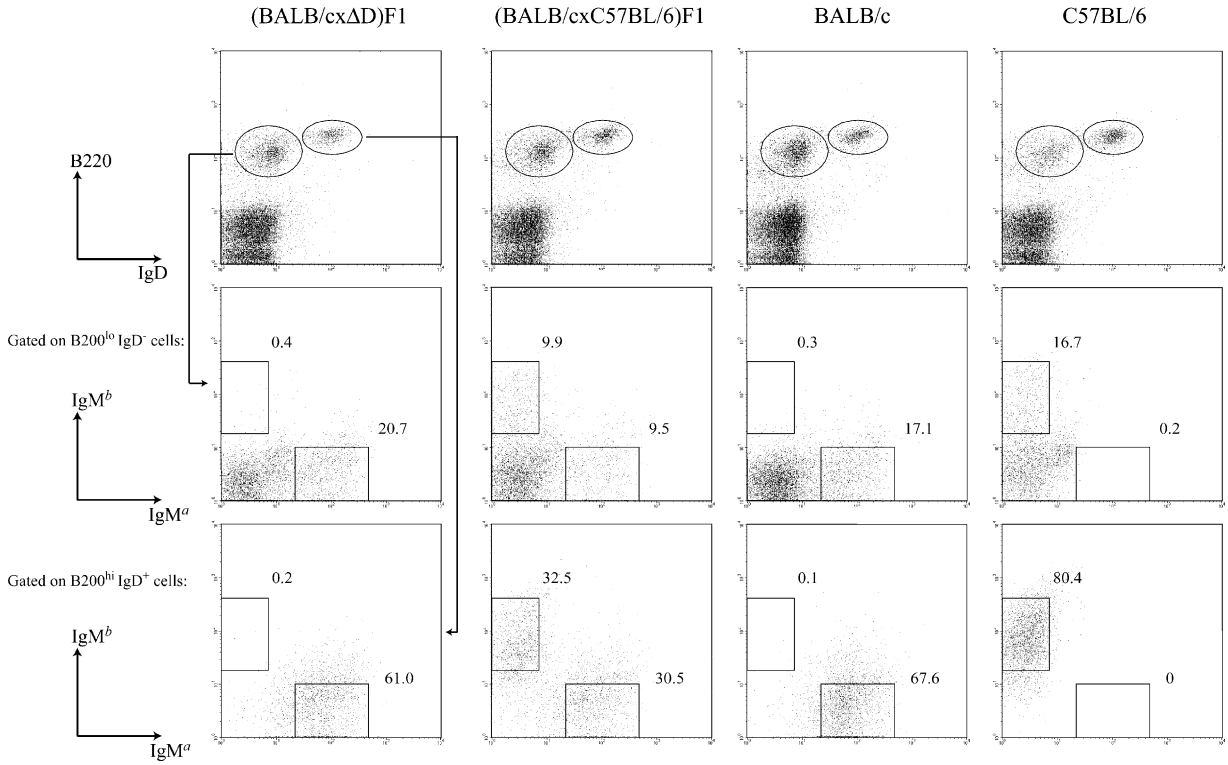

Figure 5. Absence of newly generated B cells expressing the ΔD allele in heterozygous mutant mice. Immature and mature B cells in the bone marrow of 10-mo-old (BALB/c × ΔD)F1 mice were compared with those of 5-mo-old (BALB/c × C57BL/6)F1, BALB/c, and C57BL/6 mice ($n = 2$ for each group) for expression of either IgM^a or IgM^b. The ΔD allele is of the *b* allotype, and the IgH loci of BALB/c and C57BL/6 mice are of the *a* and *b* allotype, respectively. The gated $B220^{lo}$ IgD^- population contains B cell progenitors and immature, surface IgM^+ B cells, which are analyzed for IgM allotype expression (middle). The gated $B220^{hi}$ IgD^+ population represents mature B cells, which are analyzed for IgM allotype expression (bottom).

quencing was performed at the High-throughput DNA Sequencing Facility of the Dana Farber/Harvard Cancer Center. The primers used for amplification and sequencing of V(D)J rearrangements have been described by Ehlich et al. (12) and Löffert et al. (20).

Bulk RT-PCR. RNA was extracted from sorted cells according to the TRIzol (Invitrogen) manufacturer's protocol starting with 5×10^4 cells. cDNA was prepared using the oligo-dT priming the same day. 2 μl of the cDNA was used for further amplification of the VDJ joints. Two rounds of amplification using a primer specific for the majority of mouse V_H genes MsV_HE (15) and nested constant region primers CμE and CμA (21) for the first and second rounds, correspondingly. 35 cycles were performed for each round (30 s at 97°C, 30 s at 50°C, and 30 s at 72°C). The expected 350-bp size was purified from the gel and subcloned into the TOPO TA vector (Invitrogen). DNA from individual colonies was prepared and sequenced using standard vector specific primers.

Sequence analysis of Ig rearrangements. Sequences were analyzed using www.dnaplot.de, IMGT.cines.fr, and IgBlast–based programs. The databases used consist of mouse V gene sequences from a GenBank/EMBL/

sequences in the single cell analyses, we consider the repeats in the bulk analysis an artifact resulting from the high number of amplification cycles. Two sets of sequences (1, 11 and 30, 31, 32) may represent hybrid sequences generated in the course of gene amplification by PCR (reference 27). Sequences were submitted through http://www.ncbi.nih.gov/Genbank/index.html in a consistent order (GenBank/EMBL/DDBJ accession nos. AY841948-AY841979). (B) Analysis of joints from single cell sorted and bulk sorted or MACS B cells from 5- and 10-wk-old ΔD/ΔD or WT mice. Because of space limitations, only their productive versus nonproductive status is listed. (C) CDR3 length comparison of V_HJ_H joints (excluding sequences using DST4.2) from ΔD/ΔD and ΔD/JHT B cells and $V_HD_HJ_H$ joints from WT B cells isolated from 2-, 5-, and 10-wk-old mice. Gray bars represent average number of nucleotides in the CDR3 defined as starting after the cysteine in the 3′ end of the V_H and ending with the last nucleotide before the conserved tryptophan of J_H. Error bars represent standard deviations. To demonstrate that the difference in the CDR3 length of the joints from ΔD/ΔD and WT B cells is due to the absence of D_H elements and only a single round of N and P nucleotide addition, the average length of D_H sequence in WT $V_HD_HJ_H$ joints (white bars) plus that of N/P nucleotides added in a single round (black bars) are shown on top of the CDR3 values for ΔD/ΔD sequences. The first group of bars represents a mix of sequences amplified from cDNA of 2-wk-old mice with a natural distribution of J_H usage. The second and third group is from DNA of 5-wk-old mice sequenced using a J_H4 or J_H2 primer, respectively. Because J_H element length varies, different J_H elements contribute differently to overall CDR3 length. The last bar gives the average and standard deviation for sequences derived from DNA of single cells of a 10-wk-old mouse using J_H2 primer. Sequences from appropriately age-matched WT mice were are not available. The average D_H element length in $V_HD_HJ_H$ joints was calculated from the number of nucleotides of D_H origin in the WT sequences of the corresponding group. To approximate the average number of nucleotides per one round of N/P nucleotide addition, the N/P nucleotides at the D_HJ_H and V_HD_H border in the WT joints of a corresponding group were added and divided by the number of sequences and by a factor of two.

DDBJ nucleotide sequence database, a Kabat database (22), and the V gene sequences compiled by Lefranc (23–26).

We would like to thank Drs. F. Alt and C. Bassing for stimulating and helpful discussions. We also gratefully acknowledge Drs. E. Derudder and M. Alimzhanov for critical reading of the text. The Dana-Farber/Harvard Cancer Center DNA Sequencing Facility processed sequences in a timely and efficient manner.

This work was supported by National Institutes of Health grant no. P01 AI52343.

The authors have no conflicting financial interests.

Submitted: 6 August 2004
Accepted: 29 November 2004

REFERENCES

1. Roth, D.B. 2003. Restraining the V(D)J recombinase. *Nat. Rev. Immunol.* 3:656–666.
2. Tonegawa, S. 1983. Somatic generation of antibody diversity. *Nature.* 302:575–581.
3. Jones, J.M., and M. Gellert. 2002. Ordered assembly of the V(D)J synaptic complex ensures accurate recombination. *EMBO J.* 21:4162–4171.
4. Sawchuk, D.J., F. Weis-Garcia, S. Malik, E. Besmer, M. Bustin, M.C. Nussenzweig, and P. Cortes. 1997. V(D)J recombination: modulation of RAG1 and RAG2 cleavage activity on 12/23 substrates by whole cell extract and DNA-bending proteins. *J. Exp. Med.* 185:2025–2032.
5. Schlissel, M., A. Constantinescu, T. Morrow, M. Baxter, and A. Peng. 1993. Double-strand signal sequence breaks in V(D)J recombination are blunt, 5′-phosphorylated, RAG-dependent, and cell cycle regulated. *Genes Dev.* 7:2520–2532.
6. Hochedlinger, K., and R. Jaenisch. 2002. Monoclonal mice generated by nuclear transfer from mature B and T donor cells. *Nature.* 415:1035–1038.
7. Kitamura, D., A. Kudo, S. Schaal, W. Muller, F. Melchers, and K. Rajewsky. 1992. A critical role of lambda 5 protein in B cell development. *Cell.* 69:823–831.
8. Hao, Z., and K. Rajewsky. 2001. Homeostasis of peripheral B cells in the absence of B cell influx from the bone marrow. *J. Exp. Med.* 194:1151–1164.
9. Rolink, A.G., C. Schaniel, J. Andersson, and F. Melchers. 2001. Selection events operating at various stages in B cell development. *Curr. Opin. Immunol.* 13:202–207.
10. Hayakawa, K., R.R. Hardy, A.M. Stall, and L.A. Herzenberg. 1986. Immunoglobulin-bearing B cells reconstitute and maintain the murine Ly-1 B cell lineage. *Eur. J. Immunol.* 16:1313–1316.
11. Gu, H., Y.R. Zou, and K. Rajewsky. 1993. Independent control of immunoglobulin switch recombination at individual switch regions evidenced through Cre-loxP-mediated gene targeting. *Cell.* 73:1155–1164.
12. Ehlich, A., V. Martin, W. Muller, and K. Rajewsky. 1994. Analysis of the B-cell progenitor compartment at the level of single cells. *Curr. Biol.* 4:573–583.
13. Ye, J. 2004. The immunoglobulin IGHD gene locus in C57BL/6 mice. *Immunogenetics.* 56:399–404.
14. Kepler, T.B., M. Borrero, B. Rugerio, S.K. McCray, and S.H. Clarke. 1996. Interdependence of N nucleotide addition and recombination site choice in V(D)J rearrangement. *J. Immunol.* 157:4451–4457.
15. Kantor, A.B., C.E. Merrill, L.A. Herzenberg, and J.L. Hillson. 1997. An unbiased analysis of V(H)-D-J(H) sequences from B-1a, B-1b, and conventional B cells. *J. Immunol.* 158:1175–1186.
16. Martin, F., and J.F. Kearney. 2000. B-cell subsets and the mature preimmune repertoire. Marginal zone and B1 B cells as part of a "natural immune memory". *Immunol. Rev.* 175:70–79.
17. Siebert, P.D., A. Chenchik, D.E. Kellogg, K.A. Lukyanov, and S.A. Lukyanov. 1995. An improved PCR method for walking in uncloned genomic DNA. *Nucleic Acids Res.* 23:1087–1088.
18. Forster, I., and K. Rajewsky. 1987. Expansion and functional activity of Ly-1+ B cells upon transfer of peritoneal cells into allotype-congenic, newborn mice. *Eur. J. Immunol.* 17:521–528.
19. Hooper, M., K. Hardy, A. Handyside, S. Hunter, and M. Monk. 1987. HPRT-deficient (Lesch-Nyhan) mouse embryos derived from germline colonization by cultured cells. *Nature.* 326:292–295.
20. Loffert, D., A. Ehlich, W. Muller, and K. Rajewsky. 1996. Surrogate light chain expression is required to establish immunoglobulin heavy chain allelic exclusion during early B cell development. *Immunity.* 4:133–144.
21. Sonoda, E., Y. Pewzner-Jung, S. Schwers, S. Taki, S. Jung, D. Eilat, and K. Rajewsky. 1997. B cell development under the condition of allelic inclusion. *Immunity.* 6:225–233.
22. Kabat, E.A., and T.T. Wu. 1991. Identical V region amino acid sequences and segments of sequences in antibodies of different specificities. Relative contributions of VH and VL genes, minigenes, and complementarity-determining regions to binding of antibody-combining sites. *J. Immunol.* 147:1709–1719.
23. Lefranc, M.P. 2001. IMGT, the international ImMunoGeneTics database. *Nucleic Acids Res.* 29:207–209.
24. Lefranc, M.P., V. Giudicelli, C. Ginestoux, J. Bodmer, W. Muller, R. Bontrop, M. Lemaitre, A. Malik, V. Barbie, and D. Chaume. 1999. IMGT, the international ImMunoGeneTics database. *Nucleic Acids Res.* 27:209–212.
25. Lefranc, M.P. 2003. IMGT, the international ImMunoGeneTics database. *Nucleic Acids Res.* 31:307–310.
26. Ruiz, M., V. Giudicelli, C. Ginestoux, P. Stoehr, J. Robinson, J. Bodmer, S.G. Marsh, R. Bontrop, M. Lemaitre, G. Lefranc, et al. 2000. IMGT, the international ImMunoGeneTics database. *Nucleic Acids Res.* 28:219–221.
27. Ford, J.E., M.G. McHeyzer-Williams, and M.R. Lieber. 1994. Chimeric molecules created by gene amplification interfere with the analysis of somatic hypermutation of murine immunoglobulin genes. *Gene.* 142:279–283.